

# Fast Topology-Aware Lossy Data Compression with Full Preservation of Critical Points and Local Order

Alex Fallin\*, Nathaniel Gorski†, Tripti Agarwal†, Bei Wang†, Ganesh Gopalakrishnan†, Martin Burtscher\*

\*Texas State University, USA

†University of Utah, USA

Emails: {waf13, burtscher}@txstate.edu, {gorski, beiwang}@sci.utah.edu, {tripti.agarwal@, ganesh@cs.}utah.edu

**Abstract**—Many scientific codes and instruments generate large amounts of floating-point data at high rates that must be compressed before they can be stored. Typically, only lossy compression algorithms deliver high-enough compression ratios. However, many of them provide only point-wise error bounds and do not preserve topological aspects of the data such as the relative magnitude of neighboring points. Even topology-preserving compressors tend to merely preserve some critical points and are generally slow. Our Local-Order-Preserving Compressor is the first to preserve the full local order (and thus all critical points), runs orders of magnitude faster than prior topology-preserving compressors, yields higher compression ratios than lossless compressors, and produces bit-for-bit the same output on CPUs and GPUs.

**Index Terms**—lossy data compression, critical-point preservation, local-order preservation, parallel execution

## I. INTRODUCTION

Many scientific instruments and simulations generate data volumes that far exceed what can be practically managed, both in terms of throughput and storage capacity [21]. To address this challenge, two primary compression strategies are employed: lossless and lossy. Lossless compression reproduces the original data exactly but often fails to achieve the high compression ratios required for large-scale scientific workflows. In contrast, lossy compression can provide substantially higher compression ratios depending on the chosen error bound, at the cost of discarding some information, making perfect reconstruction of the original data impossible.

Topological data analysis (TDA) employs structures such as critical points, contour trees [5], and Morse-Smale complexes [11] to describe, summarize, and analyze complex data. These topological descriptors are derived from *global* properties of the data, making the *local* guarantees provided by standard scientific data compressors insufficient for their preservation. To overcome this limitation, a variety of compressors and frameworks have been developed to preserve various topological aspects of scalar fields [17], [24], [34], [40], vector fields [25], [39], and tensor fields [16].

Unfortunately, existing topology-preserving compressors suffer from several drawbacks. First, they tend to be relatively slow: the preservation of topological information often requires substantial computation, taking orders of magnitude longer than conventional compression methods [40]. Second, most approaches preserve only limited topological information, such as the critical points on the contour tree [40]. Third,

many lossy compressors claim error control but do not strictly guarantee the error bound [15].

Our Local-Order-Preserving Compressor (LOPC) addresses these challenges by providing a strict error-bound guarantee, incorporating a new algorithm that preserves the full local order (and thus all critical points), and leveraging parallelism-friendly CPU and GPU implementations to significantly accelerate computation.

Whereas the topology of the data—defined here as the relationships among critical points—is inherently a global property, our approach focuses on preserving the relative ordering of neighboring points, referred to as the *local order*. Maintaining the local order serves as a foundational step toward preserving global topology: it improves the accuracy of local gradient flows, reduces visual artifacts such as jagged structures, and yields more accurate derived quantities.

Critical points of scalar fields (namely local minima, maxima, and saddles) are fundamental topological features that are determined entirely by the local order of the data. They serve as essential descriptors in visualization and form the basis for more complex topological constructs, such as the contour tree and the Morse-Smale complex. Moreover, critical points often carry direct physical meaning in a wide range of domains, including chemistry [4], climate science [23], and physics [35]. Because local order is defined solely from local information, it is an ideal property to preserve under lossy compression. Our method perfectly preserves the local order and, by extension, all critical points. To the best of our knowledge, no prior lossy data compressor fully preserves either property.

Since LOPC preserves more information, it compresses less than the other tested topology-preserving compressors. However, it is faster even serially. When run in parallel, it reaches speeds that are orders of magnitude higher than the related work, all while preserving local ordering, critical points, and a guaranteed error bound, a unique set of attributes among compressors in the literature.

Our main contributions include:

- **A local-order-preserving compression algorithm:** LOPC is the first algorithm that guarantees full preservation of the local order and works in combination with a guaranteed error-bounded lossy compressor.
- **Theoretical guarantees:** We show that LOPC preserves all critical-point locations and types (despite the lossy nature of

the underlying compressor), introduces no spurious critical points, and terminates.

- **Implementation and optimization:** We provide a detailed description of the implementation, optimization, and parallelization strategies used in LOPC for CPUs and GPUs.
- **Comprehensive evaluation:** We compare LOPC to 8 state-of-the-art compressors, 3 of which are topology-preserving, demonstrating its superior effectiveness in preserving critical points and local order.

Upon conclusion of the anonymization phase, our LOPC C++/OpenMP and CUDA codes will be open-sourced. The rest of this paper is organized as follows. Section II provides background. Section III summarizes related work. Section IV explains the LOPC algorithm. Section V describes the evaluation methodology. Section VI presents and discusses the results. Section VII concludes the paper with a summary.

## II. BACKGROUND

**Piecewise-Linear Scalar Fields:** LOPC targets piecewise-linear (PL) scalar functions defined on triangular (2D) or tetrahedral (3D) meshes. Let  $\mathbb{X}$  be a triangular mesh and  $f : \mathbb{X} \rightarrow \mathbb{R}$  a PL function. Then, the value of  $f$  is explicitly stored for each vertex  $v$  of  $\mathbb{X}$  and extended to all of  $\mathbb{X}$  by linear interpolation. Let  $\sigma$  be a triangular cell of  $\mathbb{X}$  with vertices  $v_1$ ,  $v_2$ , and  $v_3$ . Then, any  $x \in \sigma$  can be written uniquely in terms of its barycentric coordinates  $x = t_1v_1 + t_2v_2 + t_3v_3$ , where  $t_i \geq 0$  and  $\sum_i t_i = 1$ . We set  $f(x) = \sum_i t_i f(v_i)$ , which also holds for the analogous definition in 3D. LOPC works with scalar data defined on regular 2D and 3D grids, which it subdivides into triangular and tetrahedral meshes, respectively, as is done in prior work [37].

**Critical Points:** The critical points of a PL function  $f : \mathbb{X} \rightarrow \mathbb{R}$  are defined as follows. Let  $v \in \mathbb{X}$  be a vertex. The *link* of  $v$ ,  $Lk(v)$ , is the set of vertices of  $\mathbb{X}$  adjacent to  $v$ . The *lower link* of  $v$  is the set  $Lk^-(v) = \{v' \in Lk(v) : f(v') < f(v)\}$ . Similarly, the *upper link* is the set  $Lk^+(v) = \{v' \in Lk(v) : f(v') > f(v)\}$ . If  $Lk^-(v) = \emptyset$ , then  $v$  is a local maximum. If  $Lk^+(v) = \emptyset$ , then  $v$  is a local minimum. If  $Lk^-(v)$  and  $Lk^+(v)$  are both nonempty and contain vertices belonging to a single connected component each, then  $v$  is an ordinary (non-critical) point. Otherwise,  $v$  is a saddle point. This strategy assumes that neighboring points have different function values. We guarantee that they do using Simulation of Simplicity [12].

## III. RELATED WORK

This section describes the state-of-the-art floating-point compressors with which we compare LOPC. Note that all lossless compressors necessarily preserve the full topology.

### A. Lossless Compressors

FPzip [29] is a CPU-based library that supports both lossy and lossless compression of scientific data. It exploits floating-point data coherency to predict values in the input, computes the residuals, stores the data as integers, and uses a fast entropy encoder to achieve not only high compression ratios but also fast compression and decompression.

Zstandard [6] (ZSTD) is a parallel CPU compressor that is based on LZ77 [22], ANS [10], and Huffman [18] coding. Unlike many of the other tested compressors, ZSTD is a general-purpose compressor and does not specifically target floating-point data.

FPCompress [3] is a CPU/GPU parallel lossless floating-point compressor that targets smooth scientific data. It offers two versions for both single- and double-precision floating-point data, one that targets compression speed and one that targets compression ratio. Both speed versions use delta encoding, transformation from two's complement to magnitude sign, and leading bit elimination. The single-precision ratio version uses the same delta encoding and two's complement transformation stage but follows it with a bit shuffling step and repeated zero-byte elimination as the final step. The double-precision ratio version is similar, but a finite context method (FCM) predictor is added before the common compression pipeline. The FCM stage internally increases the data size by a factor of 2, but similar to our splitting of the bins and the subbins (see below), this increase in data size is to enable greater compression down the line. For the purpose of this work, we compare to the GPU versions of both the speed and ratio algorithms from FPCompress.

### B. Non-topology Preserving Lossy Compressors

SZ3 [26], [28], [41] is similar to its predecessor SZ2 [27] but generally produces better compression ratios with about the same throughput. It uses Lorenzo prediction [19] and dynamic spline interpolation. It also adopts entropy coding plus lossless compression after the lossy stage (e.g., Huffman [18] followed by GZIP [8] or ZSTD [7]). SZ3 is a CPU-only compressor and guarantees that the user-requested error bound will not be violated. We both directly and indirectly compare to SZ3, as it is the base compressor used in TopoA (described below). Similar to the SZ compressors, we also use quantization as a lossy step, and our lossless stages also rearrange the data but utilizing different transformations. While both LOPC and the SZ compressors are lossy, the SZ compressors do not maintain the topological information from the original file.

PFPL [13] is a high-throughput CPU and GPU compatible lossy compressor. It first quantizes the input and converts the bin values to magnitude-sign representation, but stores outliers inline rather than separately for performance reasons. It then, like LOPC, splits the input into 16kB chunks to allow for fast parallel compression. Each chunk is compressed using a pipeline of lossless data transformations. First, the data is delta encoded [20] and converted to negabinary. Second, the data is bit shuffled, similar to how it is done in ZFP. Last, the data is compressed using repeated zero-byte elimination. Like SZ3 and LOPC, PFPL guarantees that the user-requested error bound will not be violated.

### C. Topology Preserving Lossy Compressors

Several topology preserving lossy compressors for scalar field data exist. The oldest such compressor is TopoQZ [34].

It takes a single persistence parameter and focuses on preserving critical point pairs with a high persistence [36]. The decompressed data contains all pairs of critical points with a persistence above the threshold but no other critical points. Moreover, the locations of the preserved critical points may shift. Unlike TopoQZ, LOPC preserves all critical points as well as their locations. However, TopoQZ preserves persistence relationships, which LOPC does not.

TopoSZ [40] modifies SZ 1.4 [9] to preserve the contour tree [5] of the original data after persistence simplification [36]. It losslessly stores each critical point in the contour tree. For each other point, it computes upper and lower bounds based on the contour tree. It then iteratively tightens these upper and lower bounds until the contour tree of the decompressed data matches the ground truth. LOPC focuses on preserving all critical points, not just those stored in the contour tree. However, it does not ensure that the internal connections of the contour tree are preserved.

TopoA [17] is a framework designed to augment existing lossy compressors. It achieves the same goal as TopoSZ and uses a similar approach but employs a progressive strategy to tighten the upper and lower bounds. This bypasses iteratively recomputing the contour tree and boosts performance. It also introduces a more efficient quantization scheme to achieve improved compression ratios. We compare to the TopoA-augmented version of SZ3 because it is the best compressing of the augmented guaranteed-error lossy compressors.

#### IV. LOPC ALGORITHM AND IMPLEMENTATION

LOPC incorporates a modular approach to preserve the critical points and local ordering.

##### A. Quantization

The first step in LOPC is the lossy quantization. This is where the error bounding of the data occurs. LOPC supports both the point-wise absolute (ABS) error bound and the point-wise normalized absolute error bound (NOA). This means that, for an ABS error bound of  $\varepsilon$ , each value  $x$  must satisfy  $|x_{original} - x_{reconstructed}| \leq \varepsilon$ . The normalized absolute error bound is the ABS error normalized by the value range  $R = x_{max} - x_{min}$ , that is, the range between the largest and the smallest value in the input. It is commonly found in other topology preserving codes.

The quantizer uses the supplied error bound  $\varepsilon$  to map each floating-point value to a bin. This is accomplished by multiplying the value by  $1/\varepsilon$  and rounding the result to the nearest integer, which yields the bin number. Normal ABS quantization uses bins that are twice as large and decodes to the center of the bin, which is never more than  $\pm\varepsilon$  from the original value. We must halve the bin size to accommodate the later intra-bin adjustments of the reconstructed values (see below) to maintain the local ordering of the input.

In addition to the ABS quantization bins, LOPC also utilizes a set of “subbins” to adjust the values up or down in their bin range without violating the error bound. For example, with an ABS error bound of 0.1, the quantizer maps all values between

0.95 and 1.05 to bin number 10. Without subbins, all of those values would be reconstructed to 1.0. With the subbins, they are strategically reconstructed to some value between 0.95 and 1.05, all of which lie within the prescribed error bound, such that the critical-point locations and types of the input are retained as explained next.

##### B. Preserving Critical Points and Local Order

Rather than explicitly preserving critical points, LOPC iteratively corrects all values that violate the less-than relationship (i.e., local order) with their neighbors that have the same bin number. It suffices to fix only values that map to the same bin because the local ordering of values mapped to different bins is automatically preserved, as the quantization function is *monotonic increasing*. Notably, preserving local order is a stronger condition than preserving critical points; it guarantees not only the existence but also the exact types of critical points. This is accomplished using an iterative approach. Algorithm 1 shows the overall operation of LOPC, and Algorithm 2 outlines the operations of a single iteration of the local-order preservation step.

---

##### Algorithm 1 Main LOPC Operation

---

```

1: for each point  $p$  do ▷ parallel loop
2:    $p_{bin} \leftarrow$  ABS or NOA quantized input of  $p_{val}$ ;
3:    $p_{subbin} \leftarrow 0$ ;
4:    $p_{flags} \leftarrow 0$ ;
5: for each point  $p$  do ▷ parallel loop
6:   for each neighbor  $n$  of  $p$  do
7:      $p_{flags} \leftarrow p_{flags} \cup (n_{bin} = p_{bin})$ ;
8:      $p_{flags} \leftarrow p_{flags} \cup (n < p)$ ; ▷ with tie breaker
9:    $worklist1 \leftarrow$  all input points;
10: while  $worklist1$  is not empty do
11:    $worklist2 \leftarrow$  empty;
12:   Algorithm 2;
13:    $swap(worklist1, worklist2)$ ;

```

---



---

##### Algorithm 2 Parallel Subbin Computation (one iteration)

---

```

1: for each point  $p$  in  $worklist1$  do ▷ parallel loop
2:    $n_{max} \leftarrow 0$ ;
3:   for each same-bin neighbor  $n$  of  $p$  do ▷ using  $p_{flags}$ 
4:     if  $n$  should be less than  $p$  then ▷ using  $p_{flags}$ 
5:        $tie \leftarrow (n_{idx} > p_{idx})$ ; ▷ tie breaker: 0 or 1
6:        $val \leftarrow atomicRead(n_{subbin})$ ;
7:        $n_{max} \leftarrow \max(n_{max}, val + tie)$ ;
8:   if  $atomicMax(p_{subbin}, n_{max}) < n_{max}$  then
9:      $worklist2 \leftarrow worklist2 \cup \{p\}$ ’s greater same-bin neighbors};

```

---

At the outset, the subbins are zero and the original data has been binned. Then, LOPC computes a set of flags for each point  $p$  in the input. For each neighbor of  $p$ , the flags record whether the neighbor has the same bin number. If so, the flags further record whether the neighbor’s value is less

than  $p$ 's value. A deterministic tiebreaker is used to guarantee that a point is always greater or less than any neighboring point, never equal. The flags represent the ground truth that the final values must match in terms of local order.

Next, the iterative process starts. In each iteration, every point  $p$  checks its same-bin neighbors  $n$  that should be less than  $p$ , which are identified quickly by checking the flags. If they all meet the condition, nothing is done. Otherwise,  $p$ 's subbin value is set to the highest such neighbor's subbin value (or that value plus 1 if the tie breaker is in favor of the neighbor) to establish the correct less-than relationship. Note that subbin values are never decreased. This process repeats until no more changes are made, in which case it terminates.

In the end, the subbin values are as low as possible while guaranteeing the same less-than relationships in the reconstructed data as in the original data. Typically, most subbins end up with small integer values near zero, which is important for compressibility.

### C. Compression

The above computation converts each input value into two values, a bin number and a subbin number, effectively doubling the original data size. The result is two arrays holding very different information. First is the quantized bin numbers, which contain the information required to reconstruct the original data values within the requested error bound. Second is the subbin numbers, which contain the information required to recreate the original local ordering.

The information density of these two arrays varies greatly depending on the chosen error bound. For example, if the error bound is small, neighboring values tend to be mapped to distinct bins. Hence, the first array contains most of the information of the original data whereas the second array contains mostly zeros as the subbins are not needed. However, if the error bound is large, neighboring values tend to be mapped to the same bin number. In this case, the first array contains little information whereas the second array contains most of the local ordering of the data.

To boost the compression ratio, we use distinct compression algorithms for the bins and the subbins that are customized to compress the two types of data well. LOPC uses SLEEK's quantizer [1] to compute the bin numbers, which allows for guaranteed binning within the error bound without special handling of outliers. To losslessly compress the resulting bin numbers, LOPC employs the lossless portion of PFPL's compression algorithm [13], [14]. SLEEK and PFPL are effective, fast, and support both CPU and GPU execution.

To create good CPU- and GPU-parallel lossless compressors and decompressors for the subbin data, we used the LC framework [2]. For 32-bit subbins (single-precision data), it generated the 3-stage algorithm BIT\_4 RZE\_4 RZE\_1. For 64-bit subbins (double-precision data), it generated the 3-stage algorithm BIT\_8 RZE\_8 RZE\_1. In both cases, the first two stages match the word size and the final stage operates at byte granularity. The BIT stages, whose operation is outlined in Figure 1, perform a bit transposition (or bit shuffle). They

group the first bit of every value together, then all the second bits, and so on. The RZE (Repeated Zero Elimination) stages, illustrated in Figure 2, generate a bitmap in which each bit corresponds to a word in the input and indicates whether the word is zero. All zero words are then removed. The compressed output consists of the non-zero words from the input and the bitmap, which itself is repeatedly compressed with a similar algorithm that identifies repeating words rather than zero words. More detail on these stages can be found elsewhere [3].

### D. Parallelization and Optimization

LOPC uses already parallel CPU and GPU code from PFPL and SLEEK for computing, compressing, and decompressing the bin information. Moreover, it uses LC-generated CPU- and GPU-parallel lossless compressors and decompressors for the subbin data.

The subbin decoder is embarrassingly parallel as every bin/subbin pair can be independently processed to reconstruct the floating-point value. The parallelization of the subbin encoder is more involved. The flag computation (see Section IV-B) and the subbin initialization are embarrassingly parallel. The iterative phase that raises the subbin values is parallelized as follows. Each iteration runs in a separate barrier interval and increases subbins using an atomicMax operation, making the implementation lock-free. On the GPU, we assign each point to a separate thread. On the CPU, we use a blocked assignment of points to threads.

Since most points require little, if any, adjustment, many subbins reach their final value in the first few iterations. For this reason, processing every point in later iterations is often inefficient. As a remedy, LOPC employs a worklist on which it stores only the greater neighbors of a point whose subbin has just been raised so that only those points will be processed in the next iteration. Moreover, we employ two worklists, one that is read and another that is written. At the end of each iteration, we zero out the size of the old worklist and swap the pointers to the two worklists and their sizes. When filling the worklist, we use an atomicAdd to both increment the worklist size and obtain a unique slot for writing the new element. To avoid duplicates on the worklist, for each point, we record and atomically update the most recent iteration in which it was placed on the worklist.

### E. Correctness and Termination

This subsection explains how the LOPC algorithm preserves local ordering, including all critical points, while guaranteeing termination and error boundedness. Since our quantization is an increasing function, the local order is always correct between neighbors that are quantized to distinct bin numbers. Hence, in the rest of the explanation, we only consider same-bin neighbors.

Initially, all subbin numbers are zero. In each iteration, the algorithm examines, for every point, all neighbors that belong to the same bin and whose value should be lower. If a point fails the less-than relationship with any of these neighbors,

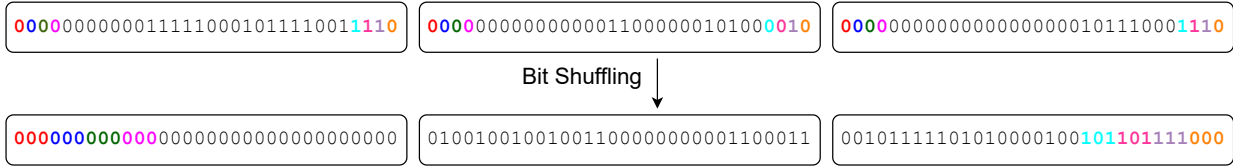


Fig. 1. Example of bit-shuffling lossless stage; for larger inputs, the sequences of bits with the same color are longer

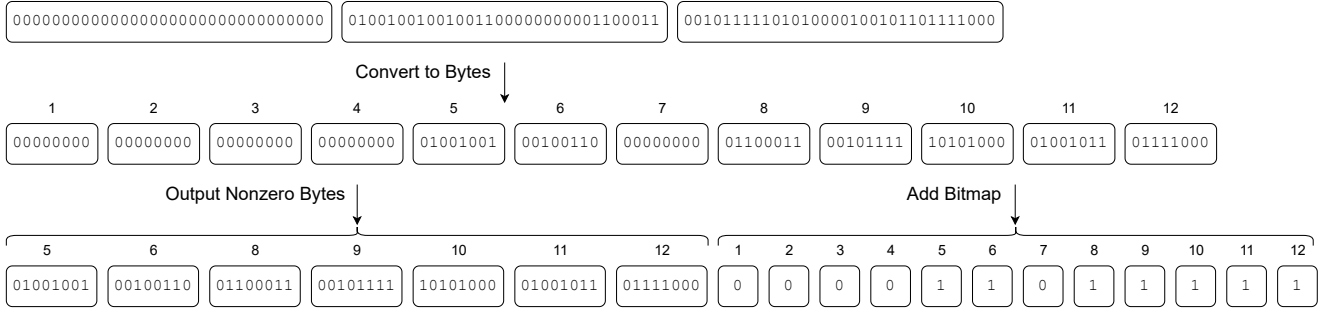


Fig. 2. Example of zero-byte elimination lossless stage; further compression of the bitmap is not shown

the subbin number of that point is raised according to one of two rules. (1) The subbin number is raised to match that of the highest violating neighbor if that neighbor’s index is lower. (2) The subbin number is raised one higher than that of the highest violating neighbor if that neighbor’s index is higher. These two rules ensure that the local ordering among neighboring points gradually becomes consistent (even in the presence of ties) with the local order of the original data.

The algorithm terminates when no violation remains, i.e., all local relationships are satisfied, thereby fully preserving the local order. Since preserving local order implies preserving local maxima, minima, and saddle points, this in turn guarantees that all critical points and their types are preserved as well.

LOPC is guaranteed to terminate because the update process is non-decreasing and bounded. In each iteration, if a violation occurs, at least one subbin number increases. This monotonicity ensures continuous progress and prevents oscillations (i.e., livelock). Moreover, the highest number a subbin can reach is finite. To see why, it helps to consider the connected component (CC) of same-bin values to which a point belongs. (1) Each such CC must contain at least one local minimum (due to the tie breaker), and the subbin number of a local minimum is never raised because it has no lower same-bin neighbors. (2) No point ever raises its subbin number to more than one higher than its highest same-bin neighbor. (3) The targeted less-than relationships are necessarily acyclic since they stem from the original input data. Together, these properties limit the possible range of subbin numbers in a CC with  $n$  points to between 0 and  $n - 1$ . Hence, after a finite number of updates, all violations disappear and the process terminates. In the worst case, when all  $n$  points form an increasing chain, the algorithm converges after  $O(n^2)$  iterations since we can create the values 0 through  $n - 1$  with  $n \times (n - 1)/2 = O(n^2)$  individual increments.

The only remaining concern is whether the subbin range

provides enough resolution to represent all necessary ordering distinctions while remaining within the quantization bin, thereby guaranteeing error boundedness. This is also guaranteed because the maximum number of subbin levels required to preserve local order within any CC is directly tied to the number of distinct floating-point values present in this CC in the original data. Note that decompression maps each value within its quantization bin such that subbin 0 decodes to the lowest representable value within the bin, subbin 1 to the next lowest, and so on. Thus, the algorithm guarantees the local order without running out of subbin range and without violating the user-provided error bound.

## V. EXPERIMENTAL METHODOLOGY

We compare LOPC to the compressors described in Section III on the two systems listed in Table I. We ran the GPU codes on System 1 and the CPU codes on System 2.

We compiled the CPU codes using the build processes supplied by their respective authors. When not specified, we used the “-O3 -march=native” flags. Unless automatically determined, the thread count was set to the number of CPU cores as hyperthreading usually does not help. We compiled the GPU codes using “-O3 -arch=sm\_89” for the RTX 4090.

For all compressors, we measured the execution time of the compression and decompression functions, excluding reading the input file, verifying the results, and transferring data to and from the device. We ran each experiment 9 times and collected the compression ratio, median compression throughput, and median decompression throughput as well as the critical-point false positives, false negatives, and false types. For all compressors, we used NOA error bounds of  $1E-2$  and  $1E-4$ . For TopoA augmented SZ3, we ran two experiments, one where the persistence threshold  $\epsilon$  is  $1.5\times$  and another where it is  $0.5\times$  the NOA error bound. These settings reflect a normal level of persistence and an over-preserving level, respectively.

If a compressor runs for more than an hour (wall-clock time), we report ‘TO’ (timeout). If a compressor crashes, fails, or runs out of memory, we report ‘DNF’ (did not finish).

TABLE I  
SYSTEMS USED FOR EXPERIMENTS

	System 1	System 2
CPU	Threadripper 2950X	Threadripper 3970X
Base Clock	3.5 GHz	3.7 GHz
Sockets	1	1
Cores Per Socket	16	32
Threads Per Core	2	2
Main memory	64 GB	256 GB
GPU	RTX 4090	N/A
Compute Capability	8.9	N/A
Base Clock	2.2 GHz	N/A
Boost Clock	2.5 GHz	N/A
SMs	128	N/A
CUDA Cores per SM	128	N/A
Main memory	24 GB HBM2e	N/A
Operating System	Fedora 37	Ubuntu 24.04.1 LTS
g++ Version	12.2.1	13.3.0
nvcc Version	12.0	N/A
GPU Driver	525.85	N/A

TABLE II  
INFORMATION ABOUT THE USED INPUTS

Name	Description	Format	Dimensions	Size (MB)
Isabel	Weather Sim.	Single	$90 \times 500 \times 500$	90
Tangaroa	Weather Sim.	Single	$300 \times 180 \times 120$	26
Earthquake	TeraShake 2 Sim.	Double	$375 \times 188 \times 50$	28
Ionization	Ionization Sim.	Double	$310 \times 128 \times 128$	41
Miranda	Hydrodynamics	Double	$384 \times 384 \times 256$	302
S3D	Weather Sim.	Double	$500 \times 500 \times 500$	1000
SCALE-LETKF	LETKF	Double	$1200 \times 1200 \times 98$	1129
QMCPACK	Quantum MC	Double	$69 \times 69 \times 115$	4

We used the 2 single- and 6 double-precision inputs listed in Table II as inputs for the compressors. The Earthquake dataset is from the TeraShake 2 earthquake simulation [30], [31]. The Ionization dataset is timestep 125 from cluster 2 of an ionization front simulation [38]. The Tangaroa dataset is the wind velocity field from a simulation of the Tangaroa research vessel [32]. The remaining inputs are sourced from the SDR-Bench repository [33], [42], which hosts real-world scientific datasets from various domains for compression evaluation. The table lists the input name, a short description, the data type, input dimensions, and file size. We chose these inputs because they are commonly used as benchmarks in topology work [17], [40] and represent the kind of scientific data that may have important topological information to preserve.

## VI. RESULTS

In this section, we evaluate the performance of the compressors discussed in Section III on the inputs described in Section V. We first discuss the preservation of critical points and local ordering for the tested compressors. Next, we compare the compression ratios achieved by each compressor using NOA error bounds. Then, we analyze the compression and decompression speed. Next, we study the effect of error bounding on the compression quality and speed. Finally,

we evaluate the reconstruction quality yielded by the tested compressors.

### A. Critical-Point and Local-Order Preservation

Table III shows the quality at which the critical points are preserved. The key strength of LOPC is immediately obvious: it preserves all critical points and local ordering whereas none of the other compressors do, not even the topology-preserving compressors. While TopoA and TopoSZ preserve the critical points on the contour tree, and TopoQZ preserves the critical point pairs, our results show the generally high number of false positives, false negatives, and false types that the other topology-preserving compressors introduce.

Comparing the other topology-preserving compressors to the non-topology-preserving lossy compressors makes it clear that a large portion of the critical points are missed when only preserving the contour tree or critical point pairs. LOPC avoids introducing any false positives, false negatives, or false types by preserving the full local ordering.

The results in the table further demonstrate that it is not straightforward for other topology-preserving compressors to preserve more critical points by lowering the persistence threshold. In many cases, doing so actually introduces more erroneous critical points in a given category. Additionally, lowering the persistence threshold introduces significant additional runtime, leading to timeouts. LOPC avoids these issues without the need for a tunable parameter.

### B. Compression Ratios

The compression ratios of the evaluated compressors across the two tested error bounds are shown in the first section of Tables IV, V, VI, and VII. Due to its CPU/GPU parity guarantee, LOPC maintains the same compression ratio across both devices.

Compared to the other compressors that maintain local order information, namely the lossless compressors (FPZip, ZSTD, and FPCompress), LOPC compresses more in all but one case. On the Ionization input with an error bound of  $1E-4$ , LOPC’s compression ratio is a little lower than that of ZSTD. In all other cases, its compression ratio is higher, on average by a factor of 3.7 and, in one case, by over a factor of 8.7.

In general, LOPC yields lower compression ratios than the other topology preserving compressors and significantly lower compression ratios than the lossy non-topology preserving compressors. This is expected for the following three reasons.

First, because LOPC preserves all local ordering, it often preserves many relationships that the other topology preserving compressors do not (see Section VI-A). Of course, it preserves even more relationships than the lossy non-topology-preserving compressors. This large amount of extra information is the main reason for the lower compression ratio.

Second, by storing bins and subbins separately, the information density of each part of the compressed file changes with the user-requested error bound. For example, if the user requests a strict error bound, most of the topological information ends up in the quantization bins, making them

TABLE III  
COUNT OF FALSE POSITIVES, FALSE NEGATIVES, AND FALSE TYPES ('M' = MILLION, 'K' = THOUSAND).

	LOPC	TopoA SZ3		TopoSZ	TopoQZ	SZ3	PFPL
		$\epsilon = 1.5x$ EB	$\epsilon = 0.5x$ EB				
EB = 1E-2							
Isabel	0/0/0	686K/16K/2K	734K/13K/3K	2M/16K/3K	461K/20K/639	28K/22K/493	430K/22K/314
Tangaroa	0/0/0	380K/2K/565	514K/2K/500	DNF	57K/4K/236	15K/5K/711	35K/7K/421
Earthquake	0/0/0	218K/95K/8K	180K/83K/8K	448K/95K/11K	22K/100K/1K	25K/110K/2K	10K/112K/398
Ionization	0/0/0	95K/12K/1K	110K/10K/1K	DNF	13K/15K/753	23K/18K/2K	16K/20K/1K
Miranda	0/0/0	1M/12M/214K	TO	644K/13M/255	566/13M/3	81K/13M/9K	2K/13M/2
S3D	0/0/0	7M/23K/5K	TO	133K/50K/218	2M/26K/2K	83K/40K/4K	2M/46K/2K
SCALE	0/0/0	4M/216K/36K	TO	8/315K/0	456K/258K/5K	268K/303K/6K	2M/310K/2K
QMCPACK	0/0/0	22K/168/34	15K/163/33	85K/313/78	11K/167/36	2K/575/16	6K/584/5
EB = 1E-4							
Isabel	0/0/0	3K/2K/162	3K/1K/132	TO	5K/4K/103	8K/5K/557	14K/8K/305
Tangaroa	0/0/0	12K/135/9	14K/128/8	70K/203/22	8K/292/15	7K/356/30	17K/540/41
Earthquake	0/0/0	183K/36K/9K	TO	199K/43K/11K	50K/41K/4K	196K/52K/13K	78K/60K/6K
Ionization	0/0/0	87K/4K/1K	118K/4K/1K	458K/4K/1K	10K/7K/814	53K/6K/1K	10K/8K/864
Miranda	0/0/0	624K/13M/74K	TO	1M/12M/779K	7/13M/0	215K/13M/22K	25/13M/0
S3D	0/0/0	27K/2K/204	TO	TO	53K/5K/295	7K/5K/409	252K/10K/715
SCALE	0/0/0	0/0/0	TO	TO	84K/129K/957	219K/155K/9K	210K/187K/3K
QMCPACK	0/0/0	122/84/16	120/84/16	268/138/25	316/119/34	135/159/25	1K/341/35

TABLE IV

COMPARISON WITH TOPOLOGY-PRESERVING COMPRESSORS FOR THE 1E-2 NOA ERROR BOUND

	LOPC			TopoA SZ3		TopoSZ	TopoQZ
	Ser	OMP	CUDA	$\epsilon = 1.5x$ EB	$\epsilon = 0.5x$ EB		
Compression Ratio							
Isabel	5.47	5.47	5.47	<b>64.40</b>	28.43	27.50	4.67
Tangaroa	4.39	4.39	4.39	<b>28.36</b>	20.91	DNF	3.33
Earthquake	8.79	8.79	8.79	<b>85.44</b>	25.09	65.85	7.08
Ionization	10.19	10.19	10.19	<b>93.45</b>	62.69	DNF	5.78
Miranda	10.05	10.05	10.05	<b>239.09</b>	TO	92.01	9.14
S3D	9.48	9.48	9.48	35.90	TO	<b>11,336.58</b>	5.82
SCALE	10.74	10.74	10.74	37.16	TO	<b>401,765.12</b>	5.82
QMCPACK	9.07	9.07	9.07	<b>102.04</b>	82.48	12.01	9.08
Geomean	8.18	8.18	8.18	68.32	37.80	<b>457.04</b>	6.04
Compression Throughput (MB/s)							
Isabel	9	17	<b>750</b>	1	1	0	14
Tangaroa	1	1	<b>104</b>	1	1	DNF	14
Earthquake	7	13	<b>940</b>	2	1	1	21
Ionization	3	4	<b>313</b>	1	1	DNF	11
Miranda	5	8	<b>414</b>	0	TO	1	8
S3D	TO	9	<b>408</b>	2	TO	2	24
SCALE	TO	TO	34	1	TO	2	<b>34</b>
QMCPACK	12	16	<b>730</b>	1	0	0	13
Geomean	5	8	<b>314</b>	1	1	0	16
Decompression Throughput (MB/s)							
Isabel	310	2,601	<b>28,754</b>	13	13	281	4
Tangaroa	316	2,592	<b>19,059</b>	11	11	DNF	4
Earthquake	441	1,896	<b>28,200</b>	15	14	564	8
Ionization	339	3,628	<b>33,305</b>	13	13	DNF	9
Miranda	422	4,314	<b>30,199</b>	10	TO	702	8
S3D	TO	3,448	<b>123,457</b>	14	TO	446	5
SCALE	TO	TO	<b>112,896</b>	14	TO	649	5
QMCPACK	429	4,380	<b>10,950</b>	13	13	438	9
Geomean	372	3,142	<b>35,229</b>	13	13	492	6

more challenging to compress easily, while the subbins contain almost no information. The reverse is true for a loose error bound because the topological information must now be stored in the subbins. This makes it difficult for a single compression algorithm to be effective in all cases due to the greatly changing information density. We discuss this relationship more in Section VI-D.

Third, LOPC is designed to work on both CPUs and GPUs. As a consequence, its compression algorithm cannot exploit some of the effective serial transformations that the CPU-only compressors include.

### C. Compression and Decompression Speed

The speeds at which the evaluated compressors compress and decompress our inputs are listed in the middle and last section of Tables IV, V, VI, and VII, respectively. The speed of the topology-preserving compressors is very input dependent.

TABLE V

COMPARISON WITH TOPOLOGY-PRESERVING COMPRESSORS FOR THE 1E-4 NOA ERROR BOUND

	LOPC			TopoA SZ3		TopoSZ	TopoQZ
	Ser	OMP	CUDA	$\epsilon = 1.5x$ EB	$\epsilon = 0.5x$ EB		
Compression Ratio							
Isabel	4.60	4.60	4.60	<b>11.92</b>	11.51	TO	2.65
Tangaroa	4.13	4.13	4.13	<b>15.49</b>	15.33	10.52	2.35
Earthquake	7.73	7.73	7.73	<b>14.51</b>	TO	6.82	4.85
Ionization	8.36	8.36	8.36	<b>33.31</b>	30.78	13.78	4.46
Miranda	8.81	8.81	8.81	<b>47.85</b>	TO	24.63	4.56
S3D	9.11	9.11	9.11	<b>51.49</b>	TO	TO	4.56
SCALE	<b>9.53</b>	<b>9.53</b>	<b>9.53</b>	2.53	TO	TO	3.98
QMCPACK	8.23	8.23	8.23	<b>39.60</b>	39.59	11.07	4.66
Geomean	7.26	7.26	7.26	19.63	<b>21.53</b>	12.19	3.89
Compression Throughput (MB/s)							
Isabel	79	8,182	<b>8,411</b>	1	1	TO	12
Tangaroa	46	199	<b>2,592</b>	1	1	0	13
Earthquake	83	470	<b>7,050</b>	2	TO	0	21
Ionization	48	102	<b>4,063</b>	2	1	0	11
Miranda	7	13	<b>643</b>	1	TO	1	8
S3D	8	568	<b>21,044</b>	3	TO	TO	22
SCALE	TO	3	<b>179</b>	1	TO	TO	31
QMCPACK	146	438	<b>4,380</b>	2	2	1	13
Geomean	38	173	<b>3,003</b>	1	1	0	15
Decompression Throughput (MB/s)							
Isabel	307	2,894	<b>31,142</b>	13	13	TO	2
Tangaroa	324	2,057	<b>27,284</b>	11	11	259	4
Earthquake	470	1,986	<b>21,793</b>	15	TO	403	6
Ionization	406	4,515	<b>29,921</b>	12	12	508	8
Miranda	425	3,355	<b>33,780</b>	10	TO	559	7
S3D	383	3,448	<b>50,618</b>	15	TO	TO	4
SCALE	TO	3,421	<b>112,896</b>	8	TO	TO	3
QMCPACK	438	4,380	<b>10,950</b>	13	12	438	8
Geomean	389	3,132	<b>32,253</b>	12	12	419	5

For example, even for LOPC, the serial and OpenMP versions time out on the SCALE input. Additionally, for the other topology-preserving compressors, the persistence threshold  $\epsilon$  has a large impact on the runtime. TopoA augmented SZ3 with a persistence threshold less than the error bound times out on 3 of the 8 inputs for the 1E-2 error bound and on 4 of the 8 inputs for the 1E-4 error bound. These results highlight the need for fast (parallelized) topology preserving compressors like LOPC. We further discuss the effect that error bound and persistence threshold have on performance in Section VI-D.

On the SCALE input at an error bound of 1E-4, only LOPC and TopoA with a large persistence threshold are able to finish within an hour. In this case, however, TopoA takes 22 minutes whereas LOPC only takes 6.3 seconds on the GPU, making it 209.9 times faster than TopoA. Further, TopoA is only able to

TABLE VI  
COMPARISON WITH NON-TOPOLOGY-PRESERVING COMPRESSORS FOR THE 1E-2 NOA ERROR BOUND

	LOPC			SZ3	PFPL	FPZip	ZSTD	FPCompress	
	Ser	OMP	CUDA					Speed	Ratio
Compression Ratio									
Isabel	5.47	5.47	5.47	<b>1,258.13</b>	33.56	2.42	1.16	1.52	1.73
Tangaroa	4.39	4.39	4.39	<b>285.80</b>	34.55	3.85	1.43	1.76	2.12
Earthquake	8.79	8.79	8.79	<b>1,336.56</b>	102.00	1.31	1.18	1.19	1.19
Ionization	10.19	10.19	10.19	<b>422.57</b>	66.92	2.26	9.50	1.47	2.89
Miranda	10.05	10.05	10.05	<b>1,350.33</b>	94.05	2.06	2.07	1.84	1.88
S3D	9.48	9.48	9.48	<b>3,097.37</b>	63.69	1.68	1.09	1.33	1.33
SCALE	10.74	10.74	10.74	<b>1,334.26</b>	120.57	1.48	2.76	1.35	1.36
QMCPACK	9.07	9.07	9.07	<b>853.99</b>	57.97	1.53	1.61	1.33	1.43
Geomean	8.18	8.18	8.18	<b>995.92</b>	65.32	1.96	1.92	1.46	1.67
Compression Throughput (MB/s)									
Isabel	9	17	750	268	229,479	96	4	<b>234,375</b>	194,805
Tangaroa	1	1	104	240	<b>207,480</b>	130	3	75,349	63,066
Earthquake	7	13	940	424	<b>166,903</b>	130	5	76,011	11,515
Ionization	3	4	313	469	<b>171,798</b>	183	1	103,390	12,209
Miranda	5	8	414	460	223,927	169	2	<b>434,518</b>	9,798
S3D	TO	9	408	456	241,723	164	2	<b>469,043</b>	9,859
SCALE	TO	TO	34	488	241,089	139	1	<b>473,557</b>	13,157
QMCPACK	12	16	730	327	<b>52,124</b>	137	6	12,959	5,566
Geomean	5	8	314	379	<b>176,190</b>	141	3	142,869	18,234
Decompression Throughput (MB/s)									
Isabel	310	2,601	28,754	644	<b>314,809</b>	60	526	201,794	143,770
Tangaroa	316	2,592	19,059	607	<b>278,159</b>	68	298	72,000	62,760
Earthquake	441	1,896	28,200	992	<b>340,120</b>	63	513	85,455	126,457
Ionization	339	3,628	33,305	1,034	<b>351,053</b>	81	726	117,775	32,821
Miranda	422	4,314	30,199	979	<b>429,901</b>	72	651	378,433	184,703
S3D	TO	3,448	123,457	979	392,667	68	792	<b>458,505</b>	210,084
SCALE	TO	TO	112,896	1,009	430,160	66	495	<b>464,975</b>	211,455
QMCPACK	429	4,380	10,950	693	<b>164,518</b>	17	17	14,504	54,752
Geomean	372	3,142	35,229	849	<b>325,142</b>	57	354	142,613	106,719

TABLE VII  
COMPARISON WITH NON-TOPOLOGY-PRESERVING COMPRESSORS FOR THE 1E-4 NOA ERROR BOUND

	LOPC			SZ3	PFPL	FPZip	ZSTD	FPCompress	
	Ser	OMP	CUDA					Speed	Ratio
Compression Ratio									
Isabel	4.60	4.60	4.60	<b>23.06</b>	6.90	2.42	1.16	1.52	1.73
Tangaroa	4.13	4.13	4.13	<b>24.49</b>	7.32	3.85	1.43	1.76	2.12
Earthquake	7.73	7.73	7.73	<b>33.99</b>	13.97	1.31	1.18	1.19	1.19
Ionization	8.36	8.36	8.36	<b>54.59</b>	16.29	2.26	9.50	1.47	2.89
Miranda	8.81	8.81	8.81	<b>81.92</b>	30.34	2.06	2.07	1.84	1.88
S3D	9.11	9.11	9.11	<b>127.02</b>	13.91	1.68	1.09	1.33	1.33
SCALE	9.53	9.53	9.53	<b>30.03</b>	20.93	1.48	2.76	1.35	1.36
QMCPACK	8.23	8.23	8.23	<b>80.89</b>	12.58	1.53	1.61	1.33	1.43
Geomean	7.26	7.26	7.26	<b>47.63</b>	13.75	1.96	1.92	1.46	1.67
Compression Throughput (MB/s)									
Isabel	79	8,182	8,411	195	225,361	96	4	<b>234,375</b>	194,805
Tangaroa	46	199	2,592	206	<b>205,793</b>	130	3	75,349	63,066
Earthquake	83	470	7,050	329	<b>162,953</b>	130	5	76,011	11,515
Ionization	48	102	4,063	384	<b>170,300</b>	183	1	103,390	12,209
Miranda	7	13	643	434	223,080	169	2	<b>434,518</b>	9,798
S3D	8	568	21,044	407	229,240	164	2	<b>469,043</b>	9,859
SCALE	TO	3	179	376	244,565	139	1	<b>473,557</b>	13,157
QMCPACK	146	438	4,380	251	<b>49,738</b>	137	6	12,959	5,566
Geomean	38	173	3,003	310	<b>172,953</b>	141	3	142,869	18,234
Decompression Throughput (MB/s)									
Isabel	307	2,894	31,142	416	<b>304,679</b>	60	526	201,794	143,770
Tangaroa	324	2,057	27,284	446	<b>275,136</b>	68	298	72,000	62,760
Earthquake	470	1,986	21,793	652	<b>335,459</b>	63	513	85,455	126,457
Ionization	406	4,515	29,921	772	<b>348,070</b>	81	726	117,775	32,821
Miranda	425	3,355	33,780	835	<b>426,173</b>	72	651	378,433	184,703
S3D	383	3,448	50,618	864	384,781	68	792	<b>458,505</b>	210,084
SCALE	TO	3,421	112,896	608	402,804	66	495	<b>464,975</b>	211,455
QMCPACK	438	4,380	10,950	602	<b>164,518</b>	17	17	14,504	54,752
Geomean	389	3,132	32,253	630	<b>318,677</b>	57	354	142,613	106,719

compress this input using the aforementioned large persistence threshold, which causes fewer critical points to be preserved on the contour tree, while LOPC is able to preserve all critical points. Serially, LOPC performs better than the other topology preserving compressors as well. This is likely due to the other compressors building a new contour tree in each iteration, a step that LOPC is able to forgo due to its entirely different approach for preserving the topology.

Naturally, LOPC is slower than the non-topology-preserving compressors, though its CUDA version is on par with some of the serial compressors. Compared to other GPU-based compressors like PFPL and FPCCompress that do not need to preserve topology, LOPC can be slower by over a factor of 100 (e.g., on the S3D input). This is expected because LOPC performs most of its topology preservation work during compression and explains why its decompression performance is much closer to the non-topology-preserving compressors.

#### D. Effects of Error Bound on LOPC Compression

The user-requested error bound affects all tested lossy compressors in terms of both compression ratio and compression/decompression speed. In this section, we discuss how each compressor behaves when the error bound is changed. Lossy compressors that do not preserve topology tend to produce significantly lower compression ratios for smaller error bounds but only incur minor slowdowns [13]. For these compressors, the computation is not directly affected by the error bound, and the slowdown stems from the increased amount of data that needs to be written due to the lower compressibility with tighter error bounds.

For the topology-preserving compressors, the compression speed is largely determined by how much correction needs to be performed. Figure 3 illustrates this for LOPC on 7 error bounds. For the loosest tested error bound, where almost all information is lost, LOPC must perform a large amount of correction and, thus, has the highest runtime. In contrast, the tightest tested error bound yields the lowest runtime because LOPC is “correcting” data that already has many of the local-order relationships intact.

Similar runtime behavior is observed in Tables IV and V for the compressors that preserve the contour tree within a persistence threshold. These compressors have an additional parameter for the persistence threshold, which also affects how much correction must be performed. In particular, more correction must be done and, therefore, more time is taken when the persistence threshold is smaller than the error bound.

Figure 3 includes LOPC’s compression ratio. The relationship between the error bound and the compression ratio is not as straightforward as the runtime relationship. The geometric-mean compression ratio is 9.3 at an error bound of 1, increases to a maximum of 10.8 at an error bound of 1E-3, and then decreases to 5.6 at the lowest error bound of 1E-6. This behavior is due to the dual-compression design of LOPC. Since LOPC processes the bins and subbins separately, there is an optimal error bound where the information is most evenly split between the bin and subbin values. TopoA behaves

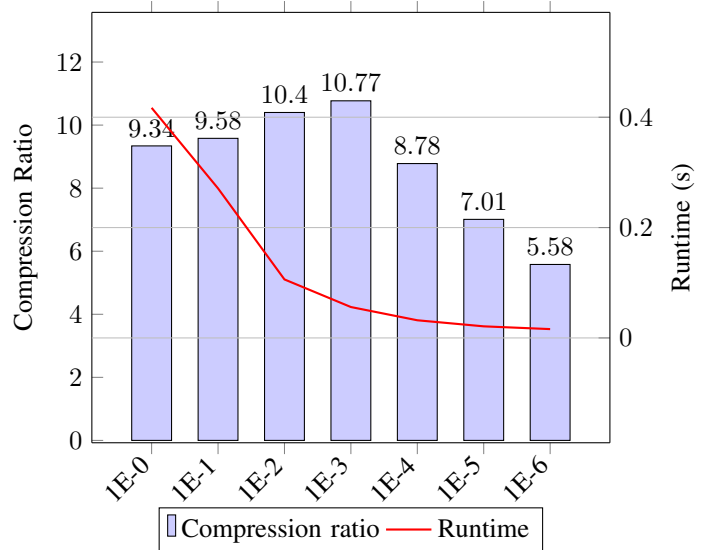


Fig. 3. Geometric-mean compression ratio and compression runtime of LOPC on 7 NOA error bounds.

similarly, where the best compressing base compressor does not always yield the highest final compression ratio [17].

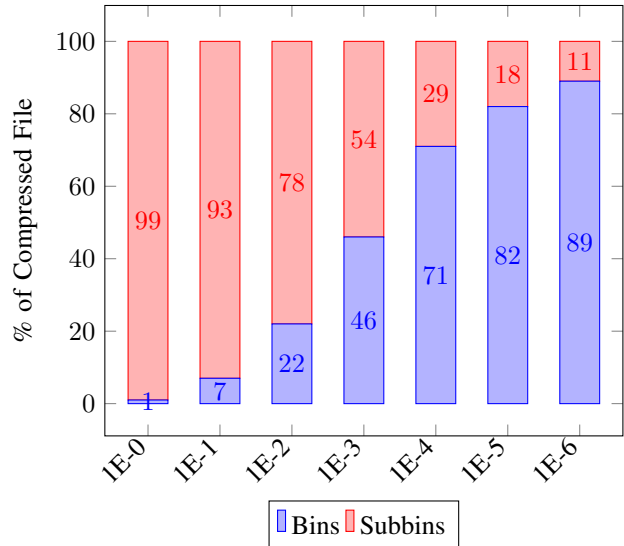


Fig. 4. Average portion of the compressed file that is bin data and subbin data for LOPC on 7 NOA error bounds.

Figure 4 shows the average fraction of the compressed file taken up by the compressed bin data and the compressed subbin data across the 7 tested error bounds. These results help explain the compression ratio results from Figure 3. As discussed, at the loosest error bound of 1, the main data (i.e., the bin information) is almost entirely lost. Hence, the bin data is extremely compressible as it contains almost no information. In contrast, the subbins contain the corrections for the main data to maintain local order. For this reason, the subbins are much less compressible and make up 99% of the compressed file. However, the overall compression ratio is still

high because the subbins only contain small numbers that are relatively easy to compress.

As the error bound decreases, the bin data starts to take up a larger portion of the compressed file. The highest observed compression ratio is seen at an error bound of  $1E-3$ , where the bins and subbins take up an approximately equal portion of the compressed file. As discussed in Section IV, we used the LC tool to generate good the compression algorithms for the bins and subbins. We targeted this search around the commonly used  $1E-3$  error bound, which contributes to the compression ratio peaking for LOPC at  $1E-3$ .

The worst compression ratios are seen at the tightest error bounds, where the bins take up most of the compressed file. This is because at these error bounds, most of the information is stored in the bins. In fact, we are approaching lossless compression with these tight error bounds, meaning most of the original floating-point information is actually retained.

In summary, all lossy compressors are affected by changes in the user-provided parameters. The non-topology-preserving lossy compressors, which tend to be memory bound, are mainly affected in compression ratio, with only a slight slowdown at lower error bounds. In contrast, the compute-bound topology-preserving compressors actually run faster at tighter error bounds, even while producing lower compression ratios, due to the decreased amount of topology correction that must be performed.

#### E. Quality of Reconstructed Data

Tables VIII and IX show the quality of the reconstructed data yielded by each tested compressor. We show peak signal-to-noise ratio (PSNR) and the structural similarity index measure (SSIM). Both are higher-is-better quality metrics that are commonly used when evaluating reconstructed lossy data.

Overall, TopoA augmented SZ3 produces the highest-quality reconstructed data, followed by LOPC. This is explained by the differences in how TopoA fixes errors compared to LOPC. When TopoA finds a topology problem, it tightens the error bound, bringing that value closer to the original, which necessarily moves the values closer to lossless encoding. This is in contrast to LOPC, which fixes problems with local ordering by monotonically increasing subbin values. This means that, while the local order is preserved, the individual values may be shifted further from their original value than traditional quantization. Even with this consideration, LOPC consistently produces higher quality reconstructions than the other topology-preserving compressors all while exceeding their speed by a large margin.

## VII. SUMMARY AND CONCLUSIONS

This paper describes LOPC, a local-order-preserving data compression algorithm. It is the first lossy compressor that fully preserves the local order (and, by extension, all critical points) of scalar fields. Moreover, it strictly guarantees the user-specified point-wise error bound.

We evaluated LOPC, three state-of-the-art topology-preserving lossy compressors, and five other leading compressors on 2 single- and 6 double-precision inputs. LOPC is

the fastest topology-preserving compressor in all cases. At the maximum, it compresses 152,000 times faster than TopoSZ. On average, is 345 times faster than TopoA-augmented SZ3 at an error bound of  $1E-4$  and a persistence threshold of  $1.5E-3$ . This speed is important for scientific simulations and instruments that produce data at high rates, where the prior state of the art in topology-preserving lossy compression is too slow to be effectively utilized.

LOPC guarantees not only the error bound, which many lossy compressors do not, but also that local ordering and all critical points are preserved. None of the prior topology-preserving compressors can do this without setting the persistence threshold to 0, which slows them down even more.

We hope that LOPC helps enable topology preservation in science where it was previously prohibitively slow to do so.

## ACKNOWLEDGMENTS

This work has been supported by the U.S. Department of Energy, Office of Science, Office of Advanced Scientific Research (ASCR), under contract DE-SC0022223.

## REFERENCES

- [1] Anju Mongandampulath Akathoott, Andrew Rodriguez, and Martin Burtscher. SLEEK: Compressing Memory Copies for Floating-Point Data on GPUs. In *2026 IEEE International Parallel and Distributed Processing Symposium (IPDPS)*, May 2026.
- [2] Noushin Azami, Alex Fallin, Brandon Burtchell, Andrew Rodriguez, Benila Jerald, Yiqian Liu, and Martin Burtscher. LC Git Repository. <https://github.com/burtscher/LC-framework>, 2025. Accessed: 2025-01-07.
- [3] Noushin Azami, Alex Fallin, and Martin Burtscher. Efficient Lossless Compression of Scientific Floating-Point Data on CPUs and GPUs. In *Proceedings of the 30th ACM International Conference on Architectural Support for Programming Languages and Operating Systems, Volume 1, ASPLOS '25*, pages 395–409, New York, NY, USA, 2025. Association for Computing Machinery.
- [4] Harsh Bhatia, Attila G Gyulassy, Vincenzo Lordi, John E Pask, Valerio Pascucci, and Peer-Timo Bremer. TopoMS: Comprehensive topological exploration for molecular and condensed-matter systems. *Journal of computational chemistry*, 39(16):936–952, 2018.
- [5] Hamish Carr, Jack Snoeyink, and Ulrike Axen. Computing contour trees in all dimensions. *Computational Geometry*, 24(2):75–94, 2003.
- [6] Yann Collet. Zstandard compression. *GitHub repository*, 2016.
- [7] Yann Collet and Murray Kucherawy. Zstandard Compression and the ‘application/zstd’ Media Type. RFC 8878, February 2021.
- [8] L. Peter Deutsch. GZIP file format specification version 4.3. RFC 1952, May 1996.
- [9] Sheng Di and Franck Cappello. Fast Error-Bounded Lossy HPC Data Compression with SZ. In *2016 IEEE International Parallel and Distributed Processing Symposium (IPDPS)*, pages 730–739, Los Alamitos, CA, USA, may 2016. IEEE Computer Society.
- [10] Jarek Duda. Asymmetric numeral systems, 2009.
- [11] Herbert Edelsbrunner, John Harer, and Afra Zomorodian. Hierarchical Morse complexes for piecewise linear 2-manifolds. In *Proceedings of the seventeenth annual symposium on Computational geometry*, pages 70–79, 2001.
- [12] Herbert Edelsbrunner and Ernst Peter Mücke. Simulation of simplicity: a technique to cope with degenerate cases in geometric algorithms. *ACM Transactions on Graphics (tog)*, 9(1):66–104, 1990.
- [13] Alex Fallin, Noushin Azami, Sheng Di, Franck Cappello, and Martin Burtscher. Fast and Effective Lossy Compression on GPUs and CPUs with Guaranteed Error Bounds. In *2025 IEEE International Parallel and Distributed Processing Symposium (IPDPS)*, pages 874–887, June 2025.
- [14] Alex Fallin, Noushin Azami, Sheng Di, Franck Cappello, and Martin Burtscher. PFPL Git Repository. <https://github.com/burtscher/PFPL>, 2025. Accessed: 2025-02-10.

TABLE VIII  
COMPARISON OF PSNR AND SSIM FOR THE 1E-2 NOA ERROR BOUND

	LOPC	TopoA SZ3		TopoSZ	TopoQZ	SZ3	PFPL
		$\epsilon = 1.5x$ EB	$\epsilon = 0.5x$ EB				
PSNR							
Isabel	52.9	55.2	<b>57.3</b>	50.4	53.0	50.8	44.8
Tangaroa	53.0	56.7	<b>58.4</b>	DNF	57.7	53.0	45.0
Earthquake	53.3	59.3	<b>63.0</b>	47.8	50.0	53.1	47.4
Ionization	51.4	54.7	<b>54.7</b>	DNF	50.0	53.9	49.2
Miranda	<b>59.9</b>	46.3	TO	41.1	49.1	54.7	52.0
S3D	56.0	62.6	TO	11.7	<b>64.4</b>	54.2	44.7
SCALE	<b>56.3</b>	49.1	TO	8.0	51.2	51.2	46.5
QMCPACK	53.1	55.3	<b>60.6</b>	49.6	51.5	47.6	44.5
Geomean	54.4	54.7	<b>58.7</b>	27.8	53.1	52.3	46.7
SSIM							
Isabel	<b>1.00</b>	<b>1.00</b>	<b>1.00</b>	<b>1.00</b>	<b>1.00</b>	<b>1.00</b>	0.97
Tangaroa	<b>1.00</b>	<b>1.00</b>	<b>1.00</b>	DNF	<b>1.00</b>	<b>1.00</b>	0.97
Earthquake	0.92	0.98	<b>0.99</b>	0.75	0.82	0.94	0.71
Ionization	<b>1.00</b>	<b>1.00</b>	<b>1.00</b>	DNF	<b>1.00</b>	<b>1.00</b>	1.00
Miranda	<b>0.31</b>	0.26	TO	0.29	0.30	0.27	0.31
S3D	0.69	0.95	TO	0.01	0.94	<b>0.98</b>	0.44
SCALE	0.62	<b>0.68</b>	TO	0.00	0.62	0.67	0.59
QMCPACK	0.99	1.00	<b>1.00</b>	0.98	0.99	0.97	0.95
Geomean	0.77	0.80	<b>1.00</b>	0.14	0.78	0.80	0.69

TABLE IX  
COMPARISON OF PSNR AND SSIM FOR THE 1E-4 NOA ERROR BOUND

	LOPC	TopoA SZ3		TopoSZ	TopoQZ	SZ3	PFPL
		$\epsilon = 1.5x$ EB	$\epsilon = 0.5x$ EB				
PSNR							
Isabel	<b>95.1</b>	94.6	94.4	TO	91.5	86.4	84.8
Tangaroa	95.1	<b>96.7</b>	96.6	90.4	90.9	87.8	84.8
Earthquake	<b>95.1</b>	94.5	TO	90.4	91.8	85.4	84.7
Ionization	95.7	97.0	<b>97.8</b>	88.7	90.5	89.4	86.4
Miranda	<b>95.6</b>	94.0	TO	83.2	89.3	89.6	90.0
S3D	92.2	<b>93.4</b>	TO	TO	91.2	89.4	84.8
SCALE	91.1	inf	TO	TO	<b>96.0</b>	86.7	84.4
QMCPACK	95.1	99.3	<b>99.3</b>	90.8	90.9	88.9	84.8
Geomean	94.3	95.6	<b>97.0</b>	88.7	91.5	87.9	85.5
SSIM							
Isabel	<b>1.00</b>	<b>1.00</b>	<b>1.00</b>	TO	<b>1.00</b>	<b>1.00</b>	<b>1.00</b>
Tangaroa	<b>1.00</b>	<b>1.00</b>	<b>1.00</b>	<b>1.00</b>	<b>1.00</b>	<b>1.00</b>	0.99
Earthquake	<b>1.00</b>	<b>1.00</b>	TO	<b>1.00</b>	<b>1.00</b>	<b>1.00</b>	1.00
Ionization	<b>1.00</b>	<b>1.00</b>	<b>1.00</b>	<b>1.00</b>	<b>1.00</b>	<b>1.00</b>	<b>1.00</b>
Miranda	<b>0.34</b>	0.30	TO	0.30	<b>0.34</b>	0.30	0.33
S3D	<b>1.00</b>	<b>1.00</b>	TO	TO	<b>1.00</b>	<b>1.00</b>	1.00
SCALE	0.81	<b>1.00</b>	TO	TO	0.86	0.85	0.76
QMCPACK	<b>1.00</b>	<b>1.00</b>	<b>1.00</b>	<b>1.00</b>	<b>1.00</b>	<b>1.00</b>	1.00
Geomean	0.85	0.86	<b>1.00</b>	0.78	0.86	0.84	0.84

- [15] Alex Fallin and Martin Burtcher. Lessons Learned on the Path to Guaranteeing the Error Bound in Lossy Quantizers, 2024.
- [16] Nathaniel Gorski, Xin Liang, Hanqi Guo, and Bei Wang. TFZ: Topology-Preserving Compression of 2D Symmetric and Asymmetric Second-Order Tensor Fields. *arXiv preprint arXiv:2508.09235*, 2025.
- [17] Nathaniel Gorski, Xin Liang, Hanqi Guo, Lin Yan, and Bei Wang. A General Framework for Augmenting Lossy Compressors with Topological Guarantees. *IEEE Transactions on Visualization and Computer Graphics*, 2025.
- [18] David A. Huffman. A Method for the Construction of Minimum-Redundancy Codes. *Proceedings of the IRE*, 40(9):1098–1101, 1952.
- [19] Lawrence Ibarria, Peter Lindstrom, Jarek Rossignac, and Andrzej Szymczak. Out-of-core Compression and Decompression of Large n-dimensional Scalar Fields. *Comput. Graph. Forum*, 22:343–348, 09 2003.
- [20] F. Jager. Delta Modulation — A Method of PCM Transmission Using the One Unit Code. *Philips Res. Repts.*, 7, 01 1952.
- [21] J. E. Kay, C. Deser, A. Phillips, A. Mai, C. Hannay, G. Strand, J. M. Arblaster, S. C. Bates, G. Danabasoglu, J. Edwards, M. Holland, P. Kushner, J.-F. Lamarque, D. Lawrence, K. Lindsay, A. Middleton, E. Munoz, R. Neale, K. Oleson, L. Polvani, and M. Vertenstein. "The Community Earth System Model (CESM) Large Ensemble Project: A Community Resource for Studying Climate Change in the Presence of Internal Climate Variability". *Bulletin of the American Meteorological Society*, 96(8):1333–1349, 2015.
- [22] Abraham Lempel and Jacob Ziv. A Universal Algorithm for Sequential Data Compression. *IEEE Transactions on Information Theory*, 23(3):337–343, May 1977.
- [23] Mingzhe Li, Dwaipayan Chatterjee, Franziska Glassmeier, Fabian Senf, and Bei Wang. Tracking Low-Level Cloud Systems with Topology. *arXiv preprint arXiv:2505.10850*, 2025.
- [24] Yuxiao Li, Xin Liang, Bei Wang, Yongfeng Qiu, Lin Yan, and Hanqi Guo. Msz: An efficient parallel algorithm for correcting morse-smale segmentations in error-bounded lossy compressors. *IEEE Transactions on Visualization and Computer Graphics*, 2024.
- [25] Xin Liang, Sheng Di, Franck Cappello, Mukund Raj, Chunhui Liu, Kenji

- Ono, Zizhong Chen, Tom Peterka, and Hanqi Guo. Toward feature-preserving vector field compression. *IEEE Transactions on Visualization and Computer Graphics*, 29(12):5434–5450, 2022.
- [26] Xin Liang, Sheng Di, Dingwen Tao, Sihuan Li, Shaomeng Li, Hanqi Guo, Zizhong Chen, and Franck Cappello. Error-Controlled Lossy Compression Optimized for High Compression Ratios of Scientific Datasets. In *2018 IEEE International Conference on Big Data (Big Data)*, pages 438–447, 2018.
- [27] Xin Liang, Sheng Di, Dingwen Tao, Sihuan Li, Shaomeng Li, Hanqi Guo, Zizhong Chen, and Franck Cappello. Error-Controlled Lossy Compression Optimized for High Compression Ratios of Scientific Datasets. In *2018 IEEE International Conference on Big Data (Big Data)*, pages 438–447, 2018.
- [28] Xin Liang, Kai Zhao, Sheng Di, Sihuan Li, Robert Underwood, Ali M. Gok, Jiannan Tian, Junjing Deng, Jon C. Calhoun, Dingwen Tao, Zizhong Chen, and Franck Cappello. SZ3: A Modular Framework for Composing Prediction-Based Error-Bounded Lossy Compressors. *IEEE Transactions on Big Data*, 9(2):485–498, 2023.
- [29] Peter Lindstrom and Martin Isenburg. Fast and efficient compression of floating-point data. *IEEE transactions on visualization and computer graphics*, 12(5):1245–1250, 2006.
- [30] K. B. Olsen, S. M. Day, J. B. Minster, Y. Cui, A. Chourasia, D. Okaya, P. Maechling, and T. Jordan. TeraShake2: Spontaneous Rupture Simulations of Mw 7.7 Earthquakes on the Southern San Andreas Fault. *Bulletin of the Seismological Society of America*, 98(3):1162–1185, 06 2008.
- [31] Mathieu Pont, Jules Vidal, Julie Delon, and Julien Tierny. Wasserstein Distances, Geodesics and Barycenters of Merge Trees. *IEEE Transactions on Visualization and Computer Graphics*, 28(1):291–301, 2022.
- [32] Stéphane Popinet, Murray Smith, and Craig Stevens. Experimental and Numerical Study of the Turbulence Characteristics of Airflow around a Research Vessel. *Journal of Atmospheric and Oceanic Technology*, 21(10):1575–1589, 2004.
- [33] SDRBench Inputs, <https://sdrbench.github.io/>, 2023.
- [34] Maxime Soler, Mélanie Plainchault, Bruno Conche, and Julien Tierny. Topologically controlled lossy compression. In *2018 IEEE Pacific Visualization Symposium (PacificVis)*, pages 46–55. IEEE, 2018.
- [35] Thierry Sousbie. The persistent cosmic web and its filamentary structure—I. Theory and implementation. *Monthly notices of the royal astronomical society*, 414(1):350–383, 2011.
- [36] Julien Tierny and Valerio Pascucci. Generalized topological simplification of scalar fields on surfaces. *IEEE transactions on visualization and computer graphics*, 18(12):2005–2013, 2012.
- [37] Jules Vidal, Pierre Guillou, and Julien Tierny. A Progressive Approach to Scalar Field Topology. *IEEE Transactions on Visualization and Computer Graphics*, 27(6):2833–2850, 2021.
- [38] Daniel Whalen and Michael L. Norman. Ionization Front Instabilities in Primordial H II Regions. *The Astrophysical Journal*, 673(2):664, feb 2008.
- [39] Mingze Xia, Bei Wang, Yuxiao Li, Pu Jiao, Xin Liang, and Hanqi Guo. TspSZ: An Efficient Parallel Error-Bounded Lossy Compressor for Topological Skeleton Preservation. In *2025 IEEE 41st International Conference on Data Engineering (ICDE)*, pages 3682–3695. IEEE Computer Society, 2025.
- [40] Lin Yan, Xin Liang, Hanqi Guo, and Bei Wang. TopoSZ: Preserving topology in error-bounded lossy compression. *IEEE Transactions on Visualization and Computer Graphics*, 30(1):1302–1312, 2023.
- [41] Kai Zhao, Sheng Di, Maxim Dmitriev, Thierry-Laurent D. Tonellot, Zizhong Chen, and Franck Cappello. Optimizing Error-Bounded Lossy Compression for Scientific Data by Dynamic Spline Interpolation. In *2021 IEEE 37th International Conference on Data Engineering (ICDE)*, pages 1643–1654, 2021.
- [42] Kai Zhao, Sheng Di, Xin Lian, Sihuan Li, Dingwen Tao, Julie Bessac, Zizhong Chen, and Franck Cappello. SDRBench: Scientific Data Reduction Benchmark for Lossy Compressors. In *2020 IEEE International Conference on Big Data (Big Data)*, pages 2716–2724, 2020.